Multiseasonal analysis of rice crop yield prediction with Sentinel-2 time series and UAV imagery in Lambayeque (Peru)

Javier A. Quille-Mamani [1*], Luis A. Ruiz [1], Lía Ramos-Fernández [2]

[1] GeoEnvironmental Cartography and Remote Sensing Group, Universitat Politècnica de València, Camí de Vera s/n, 46022,Valencia, Spain; jaquille@upv.es, laruiz@upv.es

[2] Departamento de Recursos Hídricos, Universidad Nacional Agraria La Molina, Lima, Perú; liarf@lamolina.edu.pe

Keywords: Time series, multispectral imaging, NDVI, yield prediction, precision agriculture.

Abstract

Accurate crop yield prediction is crucial for efficient agricultural and socio-economic management. Remote sensing, using satellite imagery and unmanned aerial vehicles (UAVs), provides an effective approach for yield prediction and crop monitoring, allowing time series of vegetation indices such as NDVI to be obtained and facilitating detailed analysis of crop phenology. In this study, multi-seasonality in rice yield prediction is analysed using NDVI time series obtained from Sentinel-2 (S2) and UAVs in the Lambayeque region, Peru. NDVI from S2 was extracted by applying scene classification map (SCM) masks to remove clouds and shadows. A total of 7 and 11 UAV flights were conducted during the growing season for 2022 and 2023, and yield was collected mechanically in 35 rice-producing plots. The results showed an overestimation of NDVI values obtained by UAV compared to Sentinel-2 values, as well as a significant difference in yield prediction between 2022 and 2023. In 2022, by integrating S2 and UAV NDVI series, a coefficient of determination (R^2) of 0.66 was obtained for the combination of UAV and S2, higher value than those obtained with UAV or S2 independently, with a root mean square error (RMSE) of 1.096 t/ha and a %RMSE of 10.36. In 2023, a R^2 of 0.32, a RMSE of 0.85 and a %RMSE of 9.21 were achieved. This difference is interpreted as a consequence of the cyclone *Yaku*, which caused rainfall and damage to the irrigation infrastructure, and fungi disease, leading to water stress and a decrease in yield, highlighting the importance of considering the meteorological conditions in the development of yield predictions based on NDVI series metrics obtained along the campaign.

1. Introduction

Rice is one of the most important cereals in terms of area, and more than 50% of the world's population depends on it as a primary food (Jiang et al., 2019; Sun et al., 2024). Therefore, accurate and timely yield prediction is important for yield assessment, market planning and food security monitoring. However, there are a number of complex factors that influence yield prediction, such as crop environment and weather conditions at key growth stages, which significantly impact yield (Tsujimoto et al., 2022). Climate change also affects plant metabolism and growth, with temperature and precipitation being key determinants of crop yield (Sun et al., 2024).

Satellite remote sensing data have been widely used for monitoring vegetation phenology and crop yield prediction (Sun et al., 2024). Crop yields have been estimated using different types of moderate and high-resolution satellite imagery. For example, the Moderate Resolution Imaging Spectroradiometer (MODIS) provides a temporal resolution of one to two days with a spatial resolution of 250 m to 1 km (Atzberger et al., 2013); Landsat has a nominal temporal resolution of 16 days and a spatial resolution of 30 m; and Sentinel-2 provides a higher temporal resolution of 5 days and a spatial resolution of 10-60 m, used for regional and parcel-scale monitoring. Normalised difference vegetation index (NDVI) time series have commonly been used throughout the year, mainly in environmental monitoring, agricultural forecasting, wildlife and biodiversity modelling, climate change impact assessment and drought monitoring (Mangewa et al., 2022). NDVI time series allows for the extraction of phenological metrics as independent variables to build regression models. Identifying the most reliable variables and metrics is crucial to increase the efficiency and accuracy of models, as well as to determine the point in the growing season from which models can be reliable (Bao et al., 2024).

Direct extraction of phenological metrics is hampered by noise and lack of temporal information in satellite data, due to atmospheric conditions and obstructions such as clouds and snow (Gou et al., 2019). To address this problem, data are filtered and smoothed before the extraction of phenological metrics. Several methods have been developed for this, ranging from simple linear smoothing windows to more sophisticated analytical curve functions. Most algorithms identify the beginning and end of the growing season using predefined thresholds or analytical indicators, such as the maximum curvature rate (Araya et al., 2018).

With the advancement of unmanned aerial vehicles (UAV) equipped with spectral sensors, which offer high spatial and temporal resolution, acquired data sets are less affected by external conditions. In recent years, more sophisticated operational performance and more affordable prices have been achieved. UAVs are being considered as an interesting alternative for local performance predictions. Both space-based systems and UAVs have advantages and limitations (Sun et al., 2024). Satellite imagery is cheaper, and even free, and is captured regularly, but is subject to cloud restrictions and has limited spatial resolution (Bao et al., 2024). UAVs, although more expensive, are suitable for mapping at higher resolution and detail, including intra-plot yield variability in small plots. This is crucial for correcting deficiencies in cultivation practices and for early identification of localised crop diseases and pests.

The objectives of this work are (1) to compare two rice yield prediction datasets acquired from the same area of Lambayeque, in the North of Peru: Sentinel-2 time series and UAV-based multispectral images; (2) to identify and evaluate the most efficient time series metrics for building prediction models; (2) to explore the integration of Sentinel-2 time series and UAV data acquired in strategic moments of the campaign to cover potential lacks of satellite images due to clouds or other constraints; and

(2) to compare and analyze the prediction results obtained in two field campaigns with very different regimes of rainfall and subsequent diseases.

2. Materials

2.1. Study Area.

The study area is located in the *Lambayeque* region, province of *Ferreñafe* - Peru (79º 47‘ 09.73’ W; 6º 35‘ 36.68’ S; 46 masl) (figure 1). It has a desertic climate, with deficient rainfall in all seasons, a relative humidity classified as humid (Useche et al., 2020), with temperatures ranging from 13 to 33 ºC and a total annual rainfall of about 20 mm (Quispe et al., 2024). Water supply comes from the Tinajones reservoir for the agricultural sector of the valley; however, it is scarce due to droughts and low rainfall. In addition, the region is vulnerable to extreme events such as droughts and floods related to El Niño, negatively affecting agriculture and Gross Domestic Product (GDP) (Ramírez-Juidias et al., 2024).

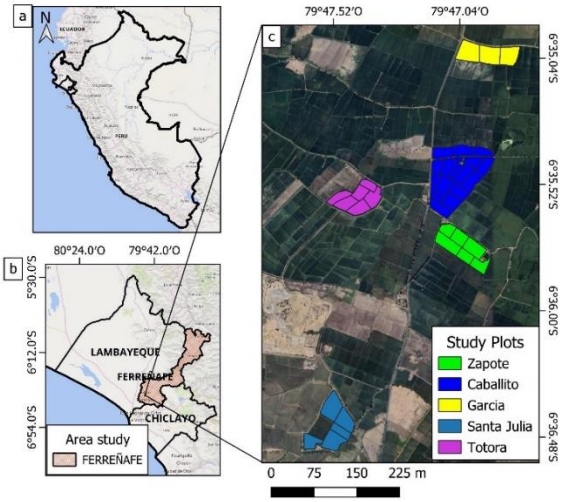

Figure 1. Geographical location of Peru (a); rice cultivation map of the study region (b) and study rice plots (c).

2.2. Field data collection

A total of 35 rice plots were harvested in 5 subareas comprising the following names: *Zapote* (FPF), *Caballito* (FSV-EC), *Garcia* (FSV-G), *Santa Julia* (FSV-SJ) and *Totora* (FSV-T) ranging in size from 5 to 12 ha per subarea. Yield data were mechanically collected by plot and weighted after harvest for the campaigns 2022 and 2023. Figure 2 shows the rice yield measured per plot for the two years considered. In general, considerably higher yield values were obtained during the 2022 campaign.

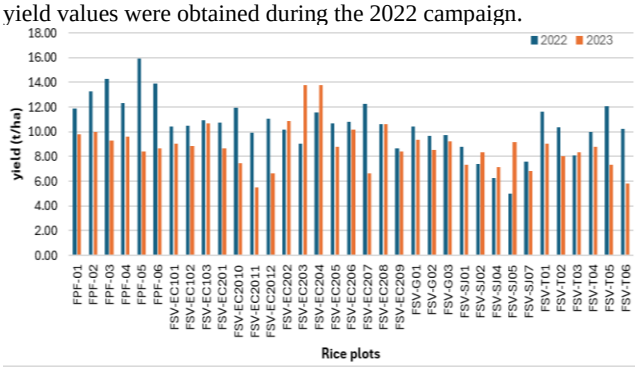

Figure 2. Rice yields as measured in the study plots for 2022 and 2023.

2.3. Meteorological data

Figure 3 shows the variation of precipitation in the study area based on data from two weather stations. Figure 3a shows the precipitation data from the Lambayeque weather station from 2020 to 2023. In contrast, figure 3b shows the 2023 precipitation from the station closest to the study area.

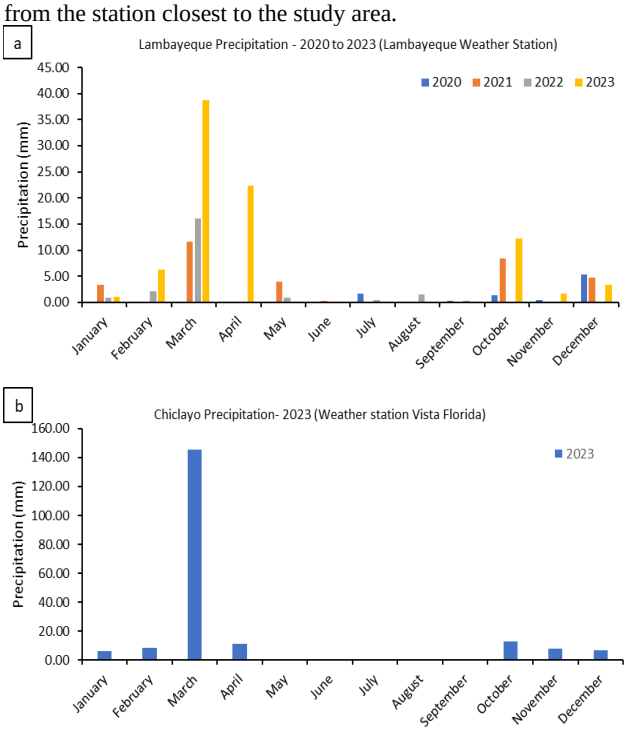

Figure 3. Evolution of annual precipitation in the study area. Annual precipitation of 2020-2023 year series from the Lambayeque station (a); and annual precipitation for 2023 from the Vista Florida station (closest to the study area) (b).

Peru's northern coastal climate is conducive to rice cultivation, making the Lambayeque region the main producer. However, it faces considerable threats from climate change. Rice is vulnerable not only to rising temperatures, water scarcity and droughts (especially during the growing season), but also to excessive flooding, particularly during the ripening phase (Useche et al., 2020). In addition, the region is vulnerable to extreme drought and rainfall events related to the El Niño (ENSO) phenomenon, which significantly affect agricultural production, resulting in a 13% decrease in Gross Domestic Product (GDP) and damage to different infrastructures (Ramírez-Juidias et al., 2024; Sandweiss and Maasch, 2022; Yglesias-González et al., 2023).

As shown in graphs of figure 3, an abrupt peak of rainfall in March 2023, due to heavy storms related to El Niño meteorological phenomenon, produced an anomalous increase of annual precipitation as compared to the regular years which were not affected by these events.

2.4. Unmanned aerial vehicle and Sentinel-2 image acquisition

UAV images were collected using a DJI Matrice 300-RTK equipped with a real-time kinematic (RTK) positioning system with a vertical and horizontal hovering accuracy of ±0.1 m in D-RTK mode, and two multispectral cameras. A Micasense RedEdge-MX (MicaSense, Inc., Seattle, WA, USA) was used in 2022 and a Parrot Sequoia (Parrot S.A., France) in 2023 campaigns, with 5 and 4 spectral bands, respectively, in the

visible, red-edge and NIR regions of the electromagnetic spectrum. Both sensors have a sunlight sensor that measures the light intensity for their corresponding spectral bands. A calibrated reflectance panel corresponding to each sensor and a sunlight sensor that automatically adjusts the readings according to the ambient illumination were used for radiometric calibration of the multispectral images (Karmakar et al., 2024). The flight plan considered a flight altitude of 120 m, a forward and lateral overlap percentage of 85 % and 80 %, respectively, and a flight speed of 8.6 m/s. A total of 7 flights were performed in 2022 and 11 flights in 2023. Image processing was carried out with Pix4Dmapper Pro software (Pix4D S.A., Prilly, Switzerland) version 4.4.12.

NDVI (Normalised Difference Vegetation Indices) time series, obtained for the 2022 and 2023 rice campaigns, were extracted from S2 imagery using the Google Earth Engine (GEE) platform, with spatial resolution of 10 m and temporal resolution of 5 days. In addition, a masking filter was applied to cloud and shadow pixels using the Scan Classification Map (SCM) provided in the S2 metadata.

3. Methods

3.1. NDVI time series interpolation, smoothing and integration

Missing NDVI time series data from S2 and UAV imagery were filled in with linear interpolation before smoothing, applying the *Savitzky-Golay* method (Chen et al., 2004; Araya et al., 2018). The Python library scipy.interpolate and scipy.signal, which includes the savgol.filter method, was used with a window_length of 8 and polyorder of 3. Since S2 images are affected by clouds and lack of data in the time series due to changing meteorological conditions, and in order to analyze the potential combination of the two data sets (S2 and UAV) to reduce these lacks in the NDVI time series of S2, both curves were integrated into one. This was performed by adjusting the available UAV curve to the S2 curve.

It was observed that the UAV NDVI data values were higher than the S2 NDVI data by, on average, 0.089 for 2022 and 0.087 for 2023. These results agree with the findings of Mangewa et al. (2022), who reported higher NDVI values for UAV compared to Sentinel-2 in the range of 0.09 to 0.20 in different habitats. S2 NDVI values are significantly affected by atmospheric conditions, unlike UAV NDVI values, which are obtained with low flight altitude and radiometric calibration (Guo et al., 2019).

Figure 4 shows the results of this integration process for a particular plot (FSV-EC207) from seeding period to harvest (day of year, DoY) as an example in both seasons for 2022 (341 DoY 2021 to 176 DoY 2022) and 2023 (336 DoY 2022 to 171 DoY 2023). Plots (a) and (d) show the original UAV (red) and S2 (blue) NDVI values as registered for the available dates, plots (b) and (e) show the result of creating the independent sensor curves and smoothing them using the *Savitzky-Golay* method, and plots (c) and (f) represent the resulting curves after the combination of both sensor curves into one.

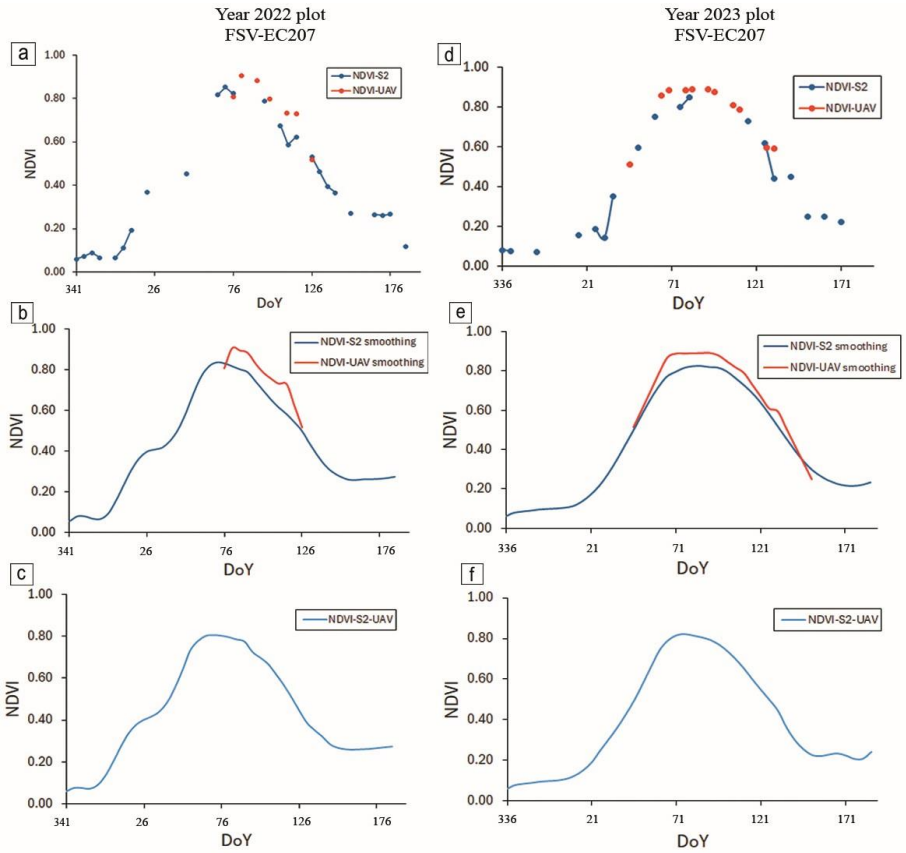

Figure 4. Example of Sentinel-2 and UAV NDVI data from seeding date to harvest (day of year, DoY) for 2022 (341 DoY 2021 to 176 DoY 2022) and 2023 (336 DoY 2022 to 171 DoY 2023) for plot FSV-EC207: Available Sentinel-2 and UAV NDVI time series values for 2022 and 2023 (a, d). Interpolated and smoothed NDVI data for 2022 and 2023 (b, e). Integrated Sentinel-2 and UAV NDVI curves for 2022 and 2023 (c, f).

3.2. Phenological metrics, prediction models generation and evaluation

Following the methodology proposed by Araya et al. (2018), a set of 15 phenological metrics were defined, such as: NDVI value at Onset (*OnsetV*), Time at Onset (*OnsetT*), Maximum NDVI value (*MaxV*), Maximum NDVI time (*MaxT*), NDVI value at Offset (*OffsetV*), Time at Offset (*OffsetT*), Length of growing season (*LengthGS*), Length of growing season before MaxT (*BeforeMaxT*), Length of growing season after MaxT (*AfterMaxT*), Growth rate between Onset and MaxT (*GreenUpSlope*), Growth rate between MaxT and Offset (*BrownDownSlope*), Area under the NDVI curve (*TINDVI*), Area under the NDVI curve between Onset and MaxT (*TINDVIBeforeMax*), Area under the NDVI curve between MaxT and Offset (*TINDVIAfterMax*), and Measure of skewness between *TINDVIBeforeMax* and *TINDVIAfterMax* (*Skewness*) (see Figure 5). These metrics were obtained from the Sentinel-2 and UAV NDVI time series for the two corresponding years. This process included a linear interpolation to fill in missing data and a smoothing process using the *Savitzky-Golay* algorithm, as described in section 3.1.

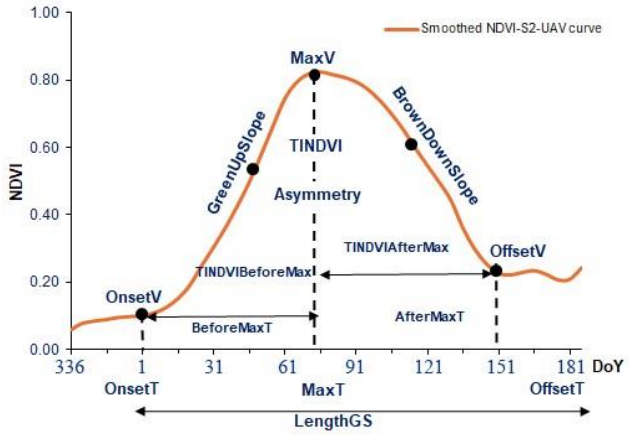

Figure 5. Smoothed NDVI-S2-UAV curve with representation of rice phenological metrics for plot FSV-EC207.

Figure 6 shows the flowchart for obtaining and evaluating the yield prediction models using S2, UAV, and combining S2-UAV imagery.

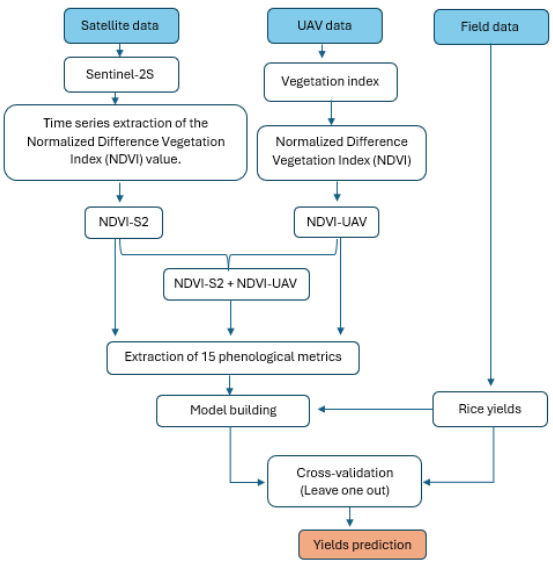

Figure 6. Flowchart for rice yield prediction.

Forward stepwise statistical multiple linear regressions were applied to select the best set of independent variables (phenological metrics) and to generate the rice yield prediction models. Leave-One-Out Cross-Validation (LOOCV) (Stone, 1974) was used to evaluate the models, computing the coefficients of determination (R^2), Root Mean Squared Error (RMSE) and Root Mean Square Error Percentage (%RMSE).

4. Results

4.1. Selected prediction variables

Table 1 shows the most relevant phenological metrics variables selected by applying forward stepwise regression. Attending to this criteria, and considering a maximum of three variables per model to avoid overfitting, for NDVI-S2 (2022) the three selected variables were: Max_Value, Offset_Time and TINDVI; for NDVI-UAV (2022) the three variables selected were Max_Time, Offset_Value and TINDVIAfterMax. For 2023, the most important variables were TINDVIBeforeMax and GreenUpSlope for NDVI-S2, while for NDVI-UAV only one variable, Offset_Time, was considered.

When NDVI of S2 and UAV were combined, only two variables were selected for 2022, Offset_Time and TINDVI, while for 2023 Max_Value, Max_Time, Offset_Value, Offset_Time and BrownDownSlope were selected (see Table 1).

Years	S2	UAV	S2+UAV
2022	Max_Value, Offset_Time and TINDVI	Max_Time, Offset_Value and TINDVIAfter Max	Offset_Time and TINDVI
2023	TINDVIBeforeMax and GreenUpSlope	Offset_Time	Max_Value, Max_Time, Offset_Value, Offset_Time, and BrownDownSlope

Table 1. Phenological metrics selected by applying forward stepwise regression as the most relevant for the models tested.

4.2. Comparative performance of prediction models

Table 2 shows the indices of model performance for campaigns 2022 and 2023, considering the three different data sets used: Sentinel-2, UAV, and a combination of both. The NDVI-S2 model for 2022 obtained R^2 of 0.6, RMSE of 1.41 t/ha, and %RMSE of 13.40%, higher than for 2023, which had R^2 of 0.30, RMSE of 0.88 t/ha, and %RMSE of 9.53%. Regarding NDVI-UAV models, the R^2 was 0.45, RMSE 1.62 t/ha, and %RMSE 15.40% for 2022, higher than for 2023, which had R^2 of 0.35, RMSE of 0.86 t/ha, and %RMSE of 9.32%. Only 21 plots were available for 2023.

In the case of the combined data set, NDVI-S2-UAV, for 2022 R^2 of 0.66, RMSE of 1.09 t/ha, and %RMSE of 10.36% were obtained, while for 2023 R^2 was 0.32, RMSE 0.85 t/ha, and %RMSE 9.21%.

Years	S2			UAV			S2+UAV		
	R^2	RMSE (t/ha)	%RMSE	R^2	RMSE (t/ha)	%RMSE	R^2	RMSE (t/ha)	%RMSE
2022	0.6	1.41	13.40	0.45	1.62	15.40	0.66	1.09	10.36
2023	0.3	0.88	9.53	0.35*	0.86*	9.32	0.32	0.85	9.21

* Only 21 plots were considered

Table 2. Linear regression model performance results using LOOCV for 2022 and 2023 using the 3 different data sets.

5. Discussion

It would be expected the selection of the same or similar phenological metrics in all cases, however, the predictor variables for each year were different. In 2022, the NDVI-S2, NDVI-UAV and NDVI-S2-UAV models had some variables in common, such as the end time of the phenological stage (*Offset_Time*) and the full integral of the NDVI curve (*TINDVI*). However, in 2023, the phenological metrics selected were different in all cases. According to some authors, the importance of the variables depends on the differences in the phenological development of the crops (Araya et al., 2018; Kong et al., 2022; Meng et al., 2014; Quille-Mamani et al., 2023). This may explain the annual differences between 2022 and 2023, which were driven by the big storms and precipitation, followed by water stress and the spread of diseases after March, 2023. These factors affected the phenological development of the rice fields (growth, flowering and ripening stages) during this campaign, and it could be the reason for the different metrics selected between seasons. On the other side, the different metrics selected in 2023 for the S2 and UAV data sets can be attributed to the small data set available for UAV, which didn’t properly get the different evolution of the NDVI curve before and after the event.

The results shown in Table 2 indicate a better prediction of the models for 2022 compared to 2023. In 2022, the results using satellite time series are similar to other studies with R^2 ranging from 0.49 to 0.66 and RMSE from 1.2 to 1.5 t/ha (Skawsang et al., 2019; Ji et al., 2022). In general, the use of UAV usually offers a clear advantage in terms of high efficiency, ease of use and spatial resolution, with R^2 ranging from 0.75 to 0.82 (Yang et al., 2022), but yield predictions may be lower (e.g., R^2 of 0.56) depending on climatic zones and potential extreme events which influence growth or reproductive stage (Yang et al., 2024).

In the first months of 2023, Peru suffered the effect of the *El Niño Costero* phenomenon, characterised by an increase in sea surface temperature on the northern coast, which caused high atmospheric temperatures, torrential rains and rivers to overflow (Yglesias-González et al., 2023). In addition, Cyclone *Yaku* affected the northern and central coast from late February to mid-March 2023, intensifying the rains caused by *El Niño Costero*. within relation to this event, the Peruvian government declared a state of emergency in the area to mitigate the consequences of the disasters (Ramos et al., 2024; Warner et al., 2024). As shown previously in Figure 3, representing precipitation in the *Lambayeque* and *Vista Florida* weather stations increased dramatically in March 2023, and these events were reflected in the anomalous low yield and phenological development of the rice crop in the study area (Figure 2). Table 2 also shows the effect of these anomalies in the models obtained for 2023, reducing the R^2 to 0.30 and 0.35 for the S2 and UAV models, respectively.

Regarding the combination of the two data sets, S2 and UAV, the results for 2022, as a meteorological stable campaign, show a slight increase of the R^2 (from 0.6 to 0.66) and a decrease of the RMSE (from 1.41 to 1.09 t/ha), even if the UAV NDVI series was not complete, but had only data in the middle and last part of the rice campaign, with discontinuities and variations depending on the plots. These results point out the opportunity of using a few UAV data acquisition at specific moments of the campaign, in order to ensure a continuity in the S2 series, filling punctual lacks of data due to clouds or other reasons, and allowing to create an integrated NDVI curve representing the complete evolution of the crop.

6. Conclusions

In this study, we compared the same methodology and datasets based on NDVI time series, from Sentinel-2 and UAV, and multiple regression linear models using phenological metrics, to estimate rice crop yielding in *Lambayeque* (Peru) in two different crop campaigns (2022 and 2023), finding important differences in terms of R^2 and RMSE of the predictive models. Whereas in 2022 the results were quite operative, in 2023 were substantially lower. This difference could be likely due to the different meteorological conditions. While 2022 was a typical dry year, with basically not rains, during 2023, and due to *El Niño* phenomenon, there were heavy rain storms and floods during the last part of the campaign, increasing the soil moisture and causing important damage in the rice plants. This change of environmental conditions could be responsible of the different behaviour of the prediction models, as well as in the different phenological metrics selected in the models for the two campaigns. In addition, the combination of two data sets, one from Sentinel-2 satellite images and the other from UAV acquisition with multispectral sensor at specific moments of the rice campaign, allows to complete the Sentinel-2 time series, slightly increasing the accuracy of the estimation and reducing the errors, which could be a potential operative approach to improve yield prediction when the relation cost-benefits allows it. Next steps of the research will be focused on obtaining more robust models for different years and campaigns, and correcting potential anomalies by including meteorological variables in the yield prediction models, such as accumulated rainfall, moisture, and others.

References

Araya, S., Ostendorf, B., Lyle, G., Lewis, M., 2018: CropPhenology: An R Package for Extracting Crop Phenology from Time Series Remotely Sensed Vegetation Index Imagery. *Ecol. Inform*., 46, 45–56.

Atzberger, C., Klisch, A., Mattiuzzi, M., Vuolo, F., 2013. Phenological metrics derived over the European continent from NDVI3g data and MODIS time series. *Remote Sensing*, 6(1), 257-284.

Bao, L., Li, X., Yu, J., Li, G., Chang, X., Yu, L., Li, Y., 2024. Forecasting spring maize yield using vegetation indices and crop phenology metrics from UAV observations. *Food and Energy Security*, 13(1), e505.

Chen, J., Jönsson, P., Tamura, M., Gu, Z., Matsushita, B., Eklundh, L., 2004. A simple method for reconstructing a high-quality NDVI time-series data set based on the Savitzky–Golay filter. *Remote sensing of Environment*, 91(3-4), 332-344.

Guo, Y., Senthilnath, J., Wu, W., Zhang, X., Zeng, Z., Huang, H., 2019. Radiometric calibration for multispectral camera of different imaging conditions mounted on a UAV platform. *Sustainability*, 11(4), 978.

Ji, Z., Pan, Y., Zhu, X., Zhang, D. , Wang, J., 2022. A generalized model to predict large-scale crop yields integrating satellite-based vegetation index time series and phenology metrics. *Ecological Indicators*, 137, 108759.

Jiang, Y., Carrijo, D., Huang, S., Chen, J., Balaine, N., Zhang, W., van Groenigen, K.J., Linquist, B., 2019: Water Management to Mitigate the Global Warming Potential of Rice Systems: A Global Meta-Analysis. *Field Crops Res*., 234, 47–54.

Karmakar, P., Teng, S.W., Murshed, M., Pang, S., Li, Y., Lin, H., 2024. Crop monitoring by multimodal remote sensing: A review. *Remote Sensing Applications: Society and Environment*, 33,101093.

Kong, D., McVicar, T.R., Xiao, M., Zhang, Y., Peña-Arancibia, J.L., Filippa, G., Xie, Y., Gu, X., 2022. phenofit: An R package for extracting vegetation phenology from time series remote sensing. *Methods in Ecology and Evolution*, 13(7), 1508-1527.

Mangewa, L.J., Ndakidemi, P.A., Alward, R.D., Kija, H.K., Bukombe, J.K., Nasolwa, E.R., Munishi, L.K., 2022. Comparative assessment of UAV and sentinel-2 NDVI and GNDVI for preliminary diagnosis of habitat conditions in Burunge wildlife management area, Tanzania. *Earth*, 3(3), 769-787.

Meng, W.A.N.G., Tao, F.L., Shi, W.J., 2014. Corn yield forecasting in northeast china using remotely sensed spectral indices and crop phenology metrics. *Journal of Integrative Agriculture*, 13(7), 1538-1545.

Quille-Mamani, J.A., Ruiz, L.A., Ramos-Fernández, L., 2023. Rice Crop Yield Prediction from Sentinel-2 Imagery Using Phenological Metric. *Environ. Sci. Proceedings*, 28(1):16.

Quispe, P.R.R., Anderson-Frey, A., McMurdie, L.A., 2024. An Index for Predicting Precipitation in the North Coast of Peru Using Logistic Regression. *Atmósfera*, 38, 721-738.

Ramírez-Juidias, E., Amaro-Mellado, J.L., Leiva-Piedra, J.L., Mediano-Guisado, J.A., 2024. Use of remote sensing techniques to infer the red globe grape variety in the Chancay-Lambayeque valley (Northern Peru). *Remote Sensing Applications: Society and Environment*, 33, 101108.

Ramos, W., Oyola-Garcia, A.E., Aguirre Gonzales, A., De la Cruz-Vargas, J.A., Luna, M., Alarcon, T., Melendez, M., Huaccho-Rojas, J., Condor-Rojas, Y.C., 2024. Time analysis of dengue deaths that occurred in two regions of Peru during the climatic-atmospheric phenomena El Nino Costero and Cyclone Yaku. *medRxiv*, 2024-03.

Sandweiss, D.H., Maasch, K.A., 2022. Climatic and cultural transitions in Lambayeque, Peru, 600 to 1540 AD: Medieval warm period to the Spanish conquest. *Geosciences*, 12(6), 238.

Skawsang, S., Nagai, M., K. Tripathi, N., Soni, P., 2019. Predicting rice pest population occurrence with satellite-derived crop phenology, ground meteorological observation, and machine learning: a case study for the Central Plain of Thailand. *Applied Sciences*, 9(22), 4846.

Stone, M., 1974. Cross-validatory choice and assessment of statistical predictions. *Journal of the Royal Statistical Soc. Series B (Methodological)*, 36(2), 111-133.

Sun, X., Zhang, P., Wang, Z., 2024. Potential of multi-seasonal vegetation indices to predict rice yield from UAV multispectral observations. *Precision Agriculture*, 1-27.

Tsujimoto, K., Kuriya, N., Ohta, T., Homma, K., Im, M.S., 2022. Quantifying the GCM-related uncertainty for climate change impact assessment of rainfed rice production in Cambodia by a combined hydrologic-rice growth model. *Ecological Modelling*, 464, 109815.

Useche P., Anglade B., Muriel J., Twyman J., 2020. Climate change in the Andes: Predictions, Perceptions and Adaptation by Peruvian Rice Farmers. Working Paper. International Center for Tropical Agriculture (CIAT), Cali, Colombia. 28.

Warner, J., Alaica, A.K., 2024. Contextualizing the influence of climate and culture on bivalve populations: Donax obesulus malacology from the north coast of Peru. *The Journal of Island and Coastal Archaeology*, 19(1), 150-171.

Yang, B., Zhu, W., Rezaei, E.E., Li, J., Sun, Z., Zhang, J., 2022. The optimal phenological phase of maize for yield prediction with high-frequency UAV remote sensing. *Remote Sensing*, 14(7), 1559.

Yang, G., Li, Y., Yuan, S., Zhou, C., Xiang, H., Zhao, Z., Wei, Q., Chen, Q., Peng, S., Xu, L., 2024. Enhancing direct-seeded rice yield prediction using UAV-derived features acquired during the reproductive phase. *Precision Agriculture*, 25(2), 1014-1037.

Yglesias-González, M., Valdés-Velásquez, A., Hartinger, S.M., Takahashi, K., Salvatierra, G., Velarde, R., Contreras, A., Santa María, H., Romanello, M., Paz-Soldán, V., Bazo, J., 2023. Reflections on the impact and response to the Peruvian 2017 Coastal El Niño event: Looking to the past to prepare for the future. *Plos one*, 18(9), e0290767.